# Management Controller for a DC MicroGrid integrating Renewables and Storages

Alessio Iovine, Gilney Damm, Elena de Santis, Maria Domenica Di Benedetto

# Management Controller for a DC MicroGrid integrating Renewables and Storages

**Alessio Iovine** [*,**] **Gilney Damm** [***] **Elena De Santis** [*]
**Maria Domenica Di Benedetto** [*]

[*] *Department of Information Engineering, Computer Science and Mathematics, Center of Excellence DEWS, University of L'Aquila, 67100 L'Aquila, Italy. (e-mail: {alessio.iovine,elena.desantis,mariadomenica.dibenedetto}@univaq.it).*
[**] *Efficacity, France (e-mail: a.iovine@efficacity.com).*
[***] *IBISC Laboratory - Paris-Saclay University, France. (e-mail: gilney.damm@ibisc.fr).*

Abstract: DC MicroGrids present an increasing interest as they represent an advantageous solution for interconnecting renewable energy sources, storage systems and loads as electric vehicles. A high-level management system able to calculate the optimal reference values for the local controllers of each of the DC MicroGrid interconnected devices is introduced in this paper. Both the changing environmental conditions and the expected load variations are taken into account. The controller considers power balance and the desired voltage level for the DC microgrid. Constraints taking into account the different nature of the storage devices are also considered.

*Keywords:* DC MicroGrid, Power management control, Optimal control, Grid stability

## 1. INTRODUCTION

To improve resilience and robustness the electricity grid is moving from its actual shape of a MacroGrid to an aggregation of MicroGrids, whose main feature is the ability to reduce the physical and electrical distance between generation and loads thanks to the integration of Distributed Generation (DG) (Farhangi (2010), Lasseter (2010)). Microgrids can be disconnected from the main grid (island mode) and have different characteristics from the existing grid; in particular, an increasing interest has been addressed in moving from the Alternate Current (AC) framework to a Direct Current (DC) one (Zubieta (2016), Dragicevic et al. (2014)). In recent years great effort is put into the development of DC microgrid dedicated control methods for the different control levels (Guerrero et al. (2011), Jimenez Carrizosa et al. (2015), Bidram et al. (2013), Dragicevic et al. (2016)) to the purpose to develop an efficient high level controller dedicated to operate power flow analysis and control.

The power flow problem is usually formulated as a nonlinear set of equations; due to computational problems a static formulation of the problem is proposed (Kundur et al. (1994), Jimenez et al. (2016), Delfino et al. (2014)).

A dynamic power flow model would be more efficient and able to schedule in real-time according to load and meteo forecasts (Bracco et al. (2015), Greenwell and Vahidi (2010), Garulli et al. (2015)). Predicted power variations could lead to a different result than the one obtained with a static model. For these reasons, thanks to the DC nature of the system we describe it as a linear set of equations that allows for a computationally fast solution of the optimal problem, inspired by Sandoval-Moreno et al. (2013)).

The target of this work is to develop a dynamic high level controller able to provide the needed references to the low level controllers that are dedicated to each physical device in the MicroGrid, considering the different limitations of each device. A DC MicroGrid integrating renewables and storages has been considered.

Selecting the right reference for a device means to properly select the needed amount of power such device must provide or absorb. Constraints regarding the nature of the devices or the physics of the grid are considered. Optimization algorithms on a power flow model are implemented in order to exactly determine the needed amount of power, while the reference for the device will be a certain level of voltage or current. So the high level controller will deal with an optimization problem on a power flow model, and then the low level controller will translate a power level into a voltage or current level.

Section 2 describes the considered hierarchical control levels. In Section 3 the mathematical model for the power flow is introduced, while in Section 4 the optimization problem is illustrated and the optimal solution is derived by using the Model Predictive Controller (MPC) technique (Camacho and Bordons (2007)). Simulation results are offered in Section 5.

## 2. HIERARCHY

The adopted hierarchical control methodology is composed by two levels:

**L**) a distributed low level control system is developed for each device composing the DC grid. The control laws operate according to the device mathematical model in order to obtain the desired level of power, which

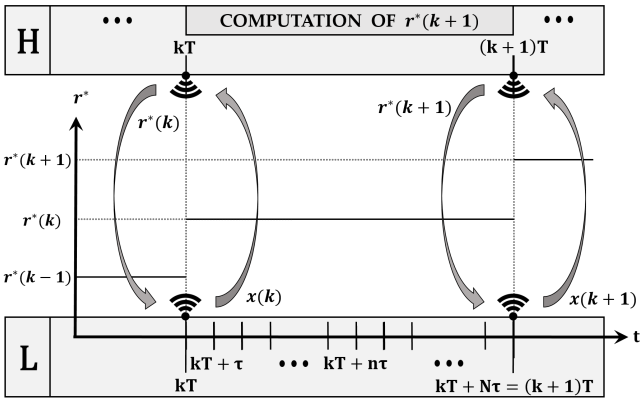


Figure 1. The adopted hierarchical control on two levels and the corresponding time scales

is a given reference (Iovine et al. (2016), Iovine et al. (2017));

**H**) a centralized high level controller provides the power references for the local low level controllers. According to a power flow model, it uses receding horizon techniques to predict the future states and calculate the optimal references to be sent to ensure power balance.

The two levels have different time scales (see Fig. 1). The low level controller (**L**) operates in a range varying from $10^{-6}$ to $10^{-3}$ seconds, while the high level one (**H**) has a range from $10^0$ to $10^1$ seconds. As shown in Fig. 1, at each high level sampling time, denoted $kT$, the controller **H** provides the references for all low level sampling times $\{kT, kT+\tau, ..., kT+n\tau, ..., kT+N\tau\}$. Note that $T = N\tau$.

At time $k-1$ the controller **H** implements a receding horizon optimization problem of a power flow model in order to predict what will be the needed power at time $k$ from all branches of the MicroGrid in order to comply with power balance. At time $k$, **H** sends the optimal reference values to the local controllers, so that they can physically let the devices obtain the requested amount of power. The value at time $k$ is based on a power flow model, on the real values of the system at time $k-1$, provided to the higher level controller by the devices operating local control and sent through a communication channel, and on the calculated system evolution over the considered prediction horizon of $\mathcal{N}$ time steps. Obviously, the iteration provides the references for $k+1$, $k+2$, etc.

*Remark 1.* The controllers do not share the state variables. Since **H** deals with a power flow model, its state will be composed by power and energy levels. On the contrary, **L** will be composed by voltages and currents. The states of **H** will be the references for **L**; indeed, given a power reference, the low level controller translates it into a voltage or current reference according to the device conditions.

*Example 1.* Given the desired power reference $P_B$ to the DC/DC converter connecting the battery to the DC grid, the low level controller converts it into a voltage reference $V^*$ according to the value of the voltage of the DC grid, $V_{DC}$, and the value of the battery voltage, $V_B$, in order to generate the current $I^*$ that is needed to provide the power $P_B$.

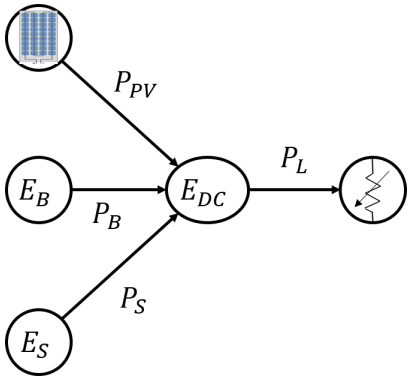


Figure 2. The considered framework in a Power Flow scheme represented as a set of nodes

## 3. POWER FLOW MODEL DESCRIPTION

A dynamic power flow model is introduced; energy variations in the devices and the power flow in a grid composed by a source, a load and two storages are considered.

### *3.1 DC Microgrid*

A DC microgrid composed by a renewable source (a photovoltaic array, PV), two storages acting at different time scale, a capacitor representing the DC grid and a load is considered (Iovine et al. (2016), Iovine et al. (2017)). Fig. 2 depicts the Microgrid as a set of energy nodes and power edges: $E_B$, $E_S$, $E_{DC}$ are the energies stored in the battery, supercapacitor and DC grid respectively, while $P_{PV}$, $P_B$, $P_S$, $P_L$ are the exchanged powers. The two storages, a battery and a supercapacitor, have different targets. The battery can be viewed as a reservoir that acts as a buffer between the flow requested by the network and the flow supplied by the production sources: its voltage is directly controlled by the DC/DC current converter applying the reference provided by the high level controller. On the contrary, the supercapacitor maintains grid voltage around a desired value: the reference value for the local controller is then not a consequence of the optimization problem but is dynamically calculated by the low level controller as a consequence of the microgrid values. The power coming/entering the supercapacitor is a consequence of the mismatch between the power produced and the power consumed. Since its target is essential for the whole grid stability, it must be able to keep doing its job. For this reason, the optimization problem will consider also the energy quantity in the supercapacitor since, if it is fully charged or discharged, it cannot keep working.

### *3.2 Assumptions*

Proper sizing of each component in a DC microgrid is an important feasibility requirement. In order to always satisfy the power requested by the load, the sizing of the PV array, battery and supercapacitor fits some conditions related to the produced power by the photovoltaic array $P_{PV}$, the $P_B$ and $P_{SC}$ power coming from the storages, and the $P_L$ power absorbed by the load:

i) *Assumption 1.* the sizing of the photovoltaic array is performed according to total energy needed in a whole day;

$$\int_0^D \overline{P}_{PV}\, dt \geq \int_0^D \overline{P}_L\, dt \tag{1}$$

where $D$ is equal to daytime (24 hours) and the quantities $\overline{P}_{PV}$, $\overline{P}_L$ represent the worst case scenario that is considered in this framework, based on previous collected data;

ii) *Assumption 2.* the sizing of the battery and the supercapacitor are performed according to the energy balance in the $T$ time step, needed for selecting a new reference;

$$\left\| \int_{kT}^{(k+1)T} (P_{PV} + P_B - P_L)\ dt \right\| \leq \tag{2}$$
$$\leq \frac{1}{2} \int_{kT}^{(k+1)T} P_{SC}\ dt \quad \forall\, k$$

The last condition can be seen as the ability of the supercapacitor to fulfill the request to provide enough amount of power in the considered time interval; for sizing the supercapacitor we consider the worst scenario due to current load variations, i.e. the case where the supercapacitor needs to provide/absorb the maximum available current for all the time steps.

*Remark 2.* The exact sizing of the components is considered out of the scope of this work.

*Assumption 3.* The variation of the load demanded power is supposed to be known, as well as the variation of the power provided by the PV array over the time we consider for prediction. Since the considered time scales are small, the corresponding small forecast errors will be dealt with by the lower level controllers.

These hypotheses are coherent with the possibility of using meteo forecast or time series analysis. Furthermore, the losses are neglected.

### *3.3 Energy Equations*

The considered models for the battery and the supercapacitor describe them as capacitors (as in Lifshitz and Weiss (2015)). The objective is to make an approximation (see Sandoval-Moreno et al. (2013)) and deal with the energy variation in the three capacitances (battery, supercapacitor and DC grid). Then, even if the energy stored in a capacitance can be calculated as

$$E = \frac{1}{2} C V^2 \tag{3}$$

where $C$ is the capacitance and $V$ the voltage, the energy variation dynamical equations are linear since we consider the voltage variation around an equilibrium value $V_0$.

Then a dynamical model can be used to describe the power flow generating the energy variations in the devices. In particular, according to the scheme in Fig. 2, the stored energy into the DC grid, the battery and the supercapacitor will have a variation depending on the power coming from the PV array, the battery, the supercapacitor and going to the load. As described by the following equations, the energy variations in the battery and the supercapacitor depend only on the power leaving or entering the devices, while for the DC grid they depend on the power balance between the produced and the demanded power. A dynamical system is obtained as

$$\begin{cases} \dot{E}_{DC} = P_{PV} + P_B + P_S - P_L \\ \dot{E}_B = -P_B \\ \dot{E}_S = -P_S \end{cases} \tag{4}$$

The model in (4) is used in Sandoval-Moreno et al. (2013) to calculate the optimal amount of power to be demanded to the battery to correctly feed a load, considering the powers as bounded control inputs or disturbances. In particular, the by the load demanded power and the one coming from the renewables are seen as disturbances and nothing can be done to modify them. We desire to examine a situation where we can deal with the capability to operate on both powers taking into account future prediction of them and physical limitations of the different storage devices. We then consider the powers as state variables: they will vary according to bounded input and disturbances in a way such that the variations are bounded according to the acting disturbances and the contemplated limitations, which are different according to the physical device.

### *3.4 Power Equations*

We describe the power variations by the following dynamical system:

$$\begin{cases} \dot{P}_{PV} = d_1 - u_1 \\ \dot{P}_L = d_2 - u_2 \\ \dot{P}_B = u_3 \\ \dot{P}_S = u_4 \end{cases} \tag{5}$$

In (5) the disturbances $d_1$ and $d_2$ are known over the considered prediction time and represent the available information we rely on to calculate the power variation (forecast, MPPT, load data). The $u_1$ control input is used to reduce the PV provided power in case it is not necessary; for example, if battery and supercapacitor are fully charged, it is necessary to curtain surplus power production. On the contrary the control input $u_2$ is needed for shedding part of the load in case the battery is fully depleted and this would be the unique solution for matching demanded and provided power (in this case the load is controllable). The inputs $u_3$ and $u_4$ are in charge for letting the power absorbed/provided by the battery and the supercapacitor vary, respectively. Due to the different nature and the different targets of the devices, they will have different characteristics.

### *3.5 Discrete Time Model*

Considering (4) and (5), it is then possible to rewrite the whole discretized dynamical system as

$$x(k+1) = A_d x(k) + B_d u(k) + D_d d(k) \tag{6}$$

where the state is

$$x = [E_{DC}\ \ E_B\ \ E_S\ \ P_{PV}\ \ P_L\ \ P_B\ \ P_S]' = \tag{7}$$
$$= [x_1\ \ x_2\ \ x_3\ \ x_4\ \ x_5\ \ x_6\ \ x_7]'$$

and the input and disturbance vectors are

$$u = [u_1\ \ u_2\ \ u_3\ \ u_4]' \tag{8}$$

$$d = [d_1\ \ d_2]' \tag{9}$$

The discrete time matrices $A_d$, $B_d$, $D_d$ are obtained with the Euler's method discretization with a sampling time $T_S$.

$$A_d = \begin{bmatrix} 1 & 0 & 0 & T_S & -T_S & T_S & T_S \\ 0 & 1 & 0 & 0 & 0 & -T_S & 0 \\ 0 & 0 & 1 & 0 & 0 & 0 & -T_S \\ 0 & 0 & 0 & 1 & 0 & 0 & 0 \\ 0 & 0 & 0 & 0 & 1 & 0 & 0 \\ 0 & 0 & 0 & 0 & 0 & 1 & 0 \\ 0 & 0 & 0 & 0 & 0 & 0 & 1 \end{bmatrix}$$

$$B_d = \begin{bmatrix} 0 & 0 & 0 & 0 \\ 0 & 0 & 0 & 0 \\ 0 & 0 & 0 & 0 \\ -T_S & 0 & 0 & 0 \\ 0 & -T_S & 0 & 0 \\ 0 & 0 & T_S & 0 \\ 0 & 0 & 0 & T_S \end{bmatrix} \qquad D_d = \begin{bmatrix} 0 & 0 \\ 0 & 0 \\ 0 & 0 \\ T_S & 0 \\ 0 & T_S \\ 0 & 0 \\ 0 & 0 \end{bmatrix}$$

## 4. PROBLEM FORMULATION

According to physical constraints, the problem we want to address is to calculate the optimal values for the power levels $P_{PV}$ ($x_4$) and $P_B$ ($x_6$) such that the demanded power $P_L$ ($x_5$) is provided, given desired energy levels for $E_{DC}$ ($x_1$), $E_B$ ($x_2$) and $E_S$ ($x_3$) in (6).

The disturbances $d_1$ and $d_2$ are supposed to be known over the considered time. Once the time interval $\mathcal{N}$ is fixed, then the vector $d$ is supposed to be known for every time $i$, $i = \{k, k+1, ..., k+\mathcal{N}\}$. $d_1$ and $d_2$ are bounded and such that a solution for the optimization problems exists in accordance to the constraints introduced in the following.

### *4.1 Constraints*

Let us now implement the physical limitations in the model. The energy time derivatives depend on physical flow considerations, assuming there are no losses. Each control law has different constraints:

- $0 \leq u_1 \leq u_1^M$, $u_1^M \geq 0$; starting from the actual value $P_{PV}(k)$ and according to the possible variation described by the disturbance $d_1$, limitations on $u_1$ allow only to reduce the power coming from the PV array;
- $0 \leq u_2 \leq u_2^M$, $u_2^M \geq 0$; as for the PV, limitations on $u_2$ allow only to reduce the load;
- $-u_3^m \leq u_3 \leq u_3^M$, $u_3^m, u_3^M \geq 0$; saving the battery life time is a priority and to this purpose limitations on the power variation are imposed;
- $-\infty \leq u_4 \leq +\infty$; since the supercapacitor has the duty to ensure voltage stability with respect to variations acting on the grid, its current derivative cannot be bounded.

Moreover, constraints must be applied to the state variables:

- $x_1^m \leq x_1 \leq x_1^M$, $x_1^m, x_1^M \geq 0$; the energy stored in the DC grid must be kept between an interval;
- $x_2^m \leq x_2 \leq x_2^M$, $x_2^m, x_2^M \geq 0$ and $x_3^m \leq x_3 \leq x_3^M$, $x_3^m, x_3^M \geq 0$; the energy in the battery and the supercapacitor must remain in a range of values, in order to not damage the devices;
- $0 \leq x_4 \leq x_4^M$, $x_4^M \geq 0$ and $0 \leq x_5 \leq x_5^M$, $x_5^M \geq 0$; the power coming from the PV array and the one consumed by the load are bounded and cannot be negative;
- $x_6^m \leq x_6 \leq x_6^M$, $x_6^m, x_6^M \geq 0$ and $x_7^m \leq x_7 \leq x_7^M$, $x_7^m, x_7^M \geq 0$; the power absorbed/provided by the battery and the supercapacitor are bounded.

The match between power in and power out is translated in a constraint as well: at every time $k$ the sum of the exchanged power must be zero, i.e.

$$x_4(k) + x_6(k) + x_7(k) - x_5(k) = 0, \ \forall k \tag{10}$$

Table 1. Initial values

| | | | |
|---|---|---|---|
| $E_{DC}(0)$ | 50 J | $E_B$ | $5 * 10^7$ J |
| $E_S(0)$ | $6 * 10^5$ J | $P_{PV}(0)$ | $3 * 10^4$ W |
| $P_L(0)$ | $5 * 10^4$ W | $P_B(0)$ | $2 * 10^4$ W |
| $P_S(0)$ | 0 W | | |

### *4.2 Target*

Let us now define a reference vector for the state. Since we have a desired voltage level for the DC grid, it is translated in a desired energy level, $E_{DC}^r = x_1^r$. The same reasoning applies to the energy in the battery and supercapacitor, i.e. there exist desired level $E_B^r = x_2^r$ and $E_S^r = x_3^r$. The best case for the battery is to have it fully charged, i.e. $x_2^r = x_2^M$. On the contrary, the best case for the supercapacitor is to ensure the maximum ability to operate on the system; it means that it must be able to absorb/provide the maximum amount of power and the best trade-off is $x_3^r = \left(x_3^m + x_3^M\right)\frac{1}{2}$. There are no references for the remaining dynamics:

$$x^r = [x_1^r \ x_2^r \ x_3^r \ 0 \ 0 \ 0 \ 0] \tag{11}$$

Let us then define $\tilde{x} = x - x^r$. The problem we want to solve is then to minimize a cost function $J$ according to the aforementioned constraints, i.e.

$$\begin{aligned} J &= \frac{1}{2}\left[\tilde{x}_{\mathcal{N}}^T P \tilde{x}_{\mathcal{N}} + \sum_{k=0}^{\mathcal{N}-1}\left(\tilde{x}_k^T Q \tilde{x}_k + u_k^T R u_k\right)\right] \\ & x(k+1) = A_d x(k) + B_d u(k) + D_d d(k), \ \forall\, k \\ & x_4(k) + x_6(k) + x_7(k) - x_5(k) = 0, \ \forall\, k \\ & x_j^m \leq x_j(k) \leq x_j^M, \ j = \{1,2,3,4,5,6,7\}, \ \forall\, k \\ & u_i^m \leq u_i(k) \leq u_i^M, \ j = \{1,2,3\}, \ \forall\, k \end{aligned} \tag{12}$$

The variation over the time of the power provided by the PV array is supposed to be governed by a known disturbance, $d_1$, and a control input $u_1$, whose target is to reduce the power. Indeed an MPPT algorithm will tell us the maximum available power, and the control input can just determine if all the power is needed or not. A similar description is valid for the time derivative of $P_L$: the disturbance $d_2$ is known according to Proposition 3 and the control input $u_2$ acts for disconnecting part of the connected load.

*Remark 3.* The state optimal trajectories obtained by the optimal control problem will be sent by **H** to **L** to let it operate grid stability. In particular, the optimal values of $P_{PV}$, $P_B$ and $P_L$ must be respected: so the low level controller will obtain its reference values from them. As explained in Section 3, the target of the supercapacitor is to maintain a fixed grid voltage level: then it does not really need of a reference power value since it automatically operates the needed action as a consequence of what the other devices do. So the value of $P_S$ is calculated only for the other devices taking it into account. The reference for the voltage level of the DC grid is supposed to be fixed a priori, so the reference coming from $E_{DC}$ is not needed.

## 5. SIMULATIONS

In this section we present simulations for the proposed model and the applied optimal control. Matlab and the optimization toolbox Yalmip (see Löfberg (2012)) have been used for obtaining such simulations.

The considered sampling time $T_S$ is one second, while the simulation time is 30 seconds. A prediction horizon of 5

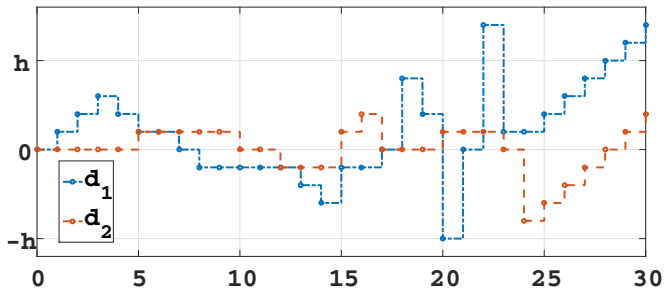


Figure 3. The considered disturbances representing the available information for photovoltaic array variation ($d_1$) and load consumption ($d_2$). The knowledge over the time is compatible with the considered prediction horizon. Here $h = 5 * 10^3$.

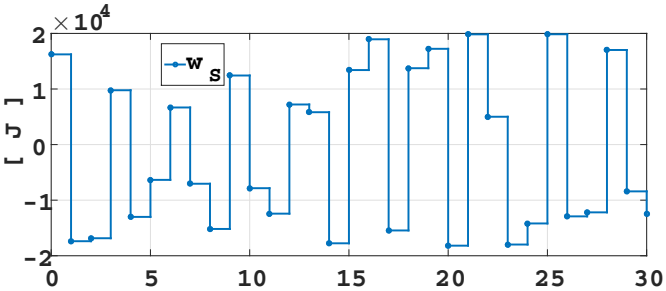


Figure 4. The considered error between the expected supercapacitor energy level and the real one over the simulation time.

time steps is utilized. Small slack variables have been used in order to relax constraints.

Fig. 3 depicts the considered disturbances $d_1$ and $d_2$, representing the available information for photovoltaic array variation and load consumption. An extra disturbance $w_s$ has also been considered at each sampling time; it takes into account and represent the difference between the considered disturbances and the real ones, acting on the supercapacitor energy level. Indeed, according to the considered low level control scheme, in case of mismatch between the provided power and the demanded one due to an error, the supercapacitor will absorb/provide power to restore power balance, increasing/reducing its energy level. Fig. 4 describes the considered energy error $w_s$ between the expected value of the supercapacitor energy level and the real one at each time step.

According to the initial values in Table 1 and to the disturbance behaviour introduced in Fig. 3, a simulation is performed to solve the problem in (12). Since the demanded power is higher than the one provided by the photovoltaic array, a contribution from the battery is expected (see Fig. 5) and consequently its energy level is expected to reduce, as seen in Fig. 6.

The level of the requested power to the battery is selected such that the demanded power by the load is fulfilled, but as well that the energy level of the DC grid and of the supercapacitor are kept constantly close to their reference values, in order to guarantee good power quality and the highest ratio of compensating actions by the supercapacitor. Fig. 7 and 8 show that the developed controller meets the targets! It must to be noticed that there are big size differences among the energy quantity that are stored in the different devices.

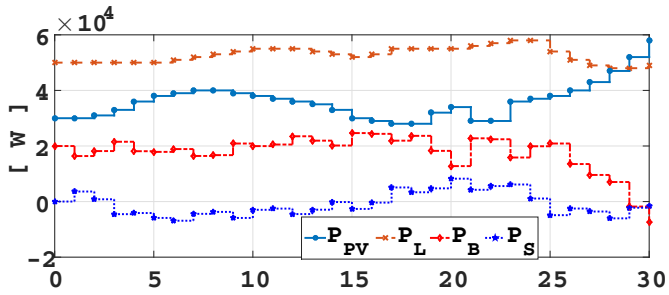


Figure 5. The power $P_{PV}$ provided by the PV array; the power $P_L$ demanded by the load; the power provided/absorbed by the battery $P_B$ and the supercapacitor $P_S$.

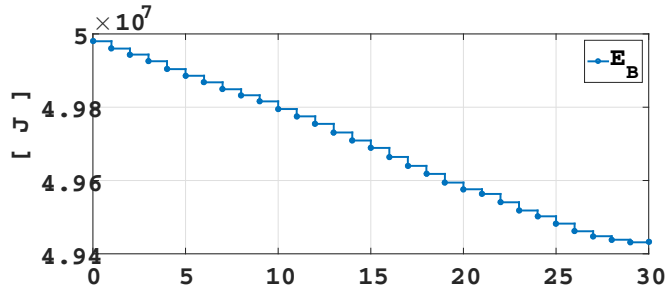


Figure 6. The energy $E_B$ of the battery.

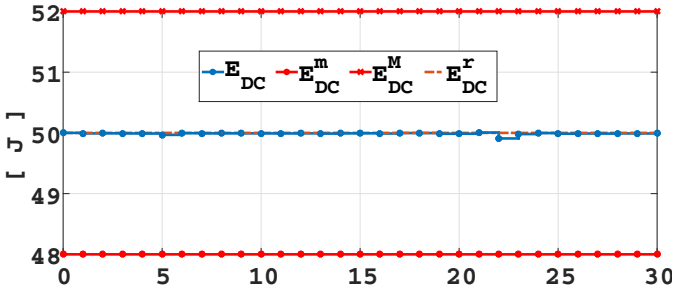


Figure 7. The energy $E_{DC}$ of the DC grid, its constraints $E^m_{DC}$, $E^M_{DC}$ and its reference value $E^r_{DC}$.

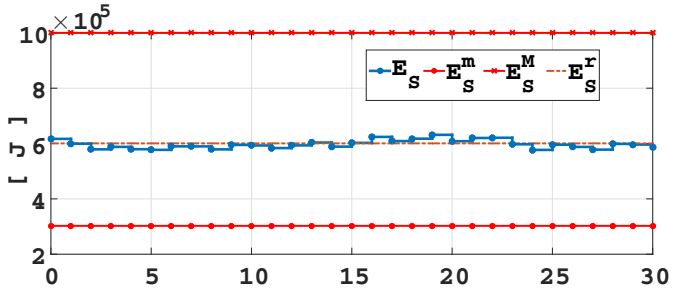


Figure 8. The energy $E_S$ of the supercapacitor, its constraints $E^m_S$, $E^M_S$ and its reference value $E^r_S$.

As confirmation of the good quality of the obtained results, the sum of all the exchanged powers is introduced in Fig. 9. Ideally, it is supposed to be zero (see condition (10)); since there is an error with magnitude $10^{-1}$ in respect to powers of $10^4$ $W$, it can be neglected.

Fig. 10 depicts the optimal control inputs that have been calculated to meet the targets. Since the power coming from the PV was not enough to feed the load, the control input $u_1$ which is dedicated to cut the exceeding power coming from the PV has always a value equal to zero. The same value is obtained for the control input $u_2$, since there is no need to cut part of the load since the battery had

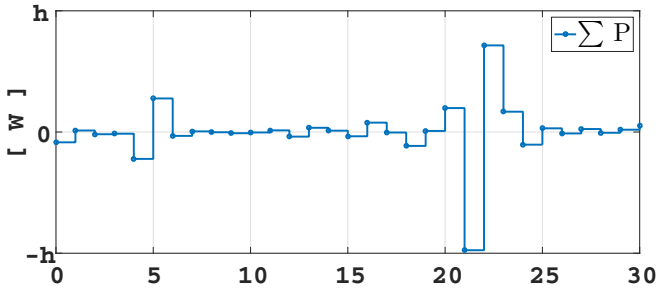


Figure 9. The sum of the exchanged powers ($h = 10^{-1}$).

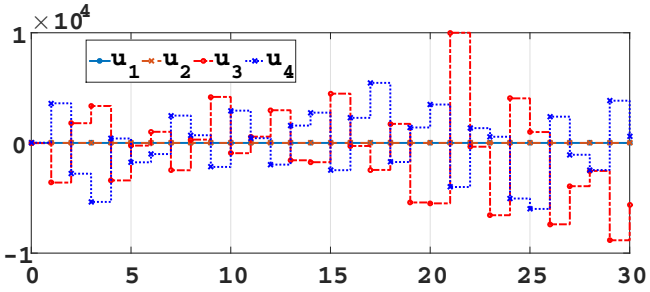


Figure 10. The optimal control inputs $u_1$, $u_2$, $u_3$ and $u_4$ calculated according to the described targets.

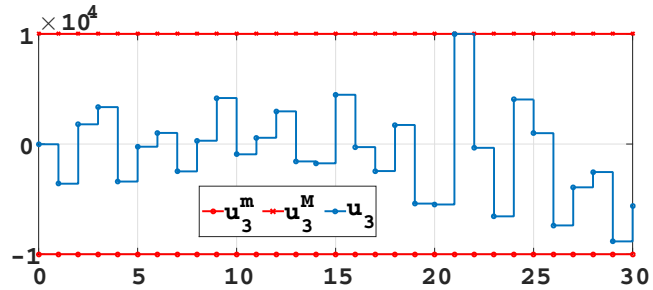


Figure 11. The optimal control input $u_3$ calculated according to the described targets. It must to be noticed that it is always inside the constrained area.

enough power and the demanded power variations were inside the constraints (see Fig. 11).

Finally it is possible to state that the developed high level controller fit the target to describe and predict the power flow of a DC MicroGrid and then the obtained power values can be used by the low level controller as references to ensure grid stability.

## 6. CONCLUSIONS

A dynamic power flow model is introduced to calculate the references the low level controller needs to ensure grid stability, both in voltage and power balance sense. A receding horizon technique is utilized in order to use prediction of the disturbances acting on the system and to let the state variables reach the desired values.

The developed model allows to take into account the different nature and characteristics of the different physical devices and to use current and predicted information about load or power coming from renewables. The results show that the control strategy correctly fits the target to describe and predict the power flow of a DC MicroGrid and then that the obtained power values can be used by the low level controller as references to ensure grid stability.

Future work will regard the extension to the case of interconnection among multiple DC microgrids.

## REFERENCES


Bidram, A., Davoudi, A., Lewis, F.L., and Guerrero, J.M. (2013). Distributed Cooperative Secondary Control of Microgrids Using Feedback Linearization. *IEEE Transactions on Power Systems*, 28(3), 3462–3470. doi:10.1109/tpwrs.2013.2247071.

Bracco, S., Delfino, F., Pampararo, F., Robba, M., and Rossi, M. (2015). A dynamic optimization-based architecture for polygeneration microgrids with tri-generation, renewables, storage systems and electrical vehicles. *Energy Conversion and Management*, 96, 511 – 520.

Camacho, E.F. and Bordons, C. (2007). *Model predictive control*.

Delfino, F., Minciardi, R., Pampararo, F., and Robba, M. (2014). A Multilevel Approach for the Optimal Control of Distributed Energy Resources and Storage. *IEEE Transactions on Smart Grid*, 5(4), 2155–2162.

Dragicevic, T., Lu, X., Vasquez, J., and Guerrero, J. (2016). DC Microgrids-Part II: A Review of Power Architectures, Applications, and Standardization Issues. *Power Electronics, IEEE Transactions on*, 31(5), 3528–3549.

Dragicevic, T., Vasquez, J., Guerrero, J., and Skrlec, D. (2014). Advanced LVDC Electrical Power Architectures and Microgrids: A step toward a new generation of power distribution networks. *Electrification Magazine, IEEE*, 2(1), 54–65.

Farhangi, H. (2010). The path of the smart grid. *Power and Energy Magazine, IEEE*, 8(1), 18–28. doi:10.1109/MPE.2009.934876.

Garulli, A., Paoletti, S., and Vicino, A. (2015). Models and Techniques for Electric Load Forecasting in the Presence of Demand Response. *IEEE Transactions on Control Systems Technology*, 23(3), 1087–1097. doi:10.1109/TCST.2014.2361807.

Greenwell, W. and Vahidi, A. (2010). Predictive Control of Voltage and Current in a Fuel Cell-Ultracapacitor Hybrid. *IEEE Transactions on Industrial Electronics*, 57(6), 1954–1963.

Guerrero, J., Vasquez, J., Matas, J., de Vicua, L., and Castilla, M. (2011). Hierarchical Control of Droop-Controlled AC and DC Microgrids; A General Approach Toward Standardization. *Industrial Electronics, IEEE Transactions on*, 58(1), 158–172.

Iovine, A., Siad, S.B., Damm, G., De Santis, E., and Di Benedetto, M.D. (2016). Nonlinear control of an AC-connected DC microgrid. In *Industrial Electronics Society, IECON 2016 - 42nd Annual Conference of the IEEE*.

Iovine, A., Siad, S.B., Damm, G., De Santis, E., and Di Benedetto, M.D. (2017). Nonlinear control of a dc microgrid for the integration of photovoltaic panels. *IEEE Transactions on Automation Science and Engineering*, 14(2), 524–535.

Jimenez, E., Carrizosa, M.J., Benchaib, A., Damm, G., and Lamnabhi-Lagarrigue, F. (2016). A new generalized power flow method for multi connected DC grids. *International Journal of Electrical Power and Energy Systems*, 74, 329 – 337.

Jimenez Carrizosa, M., Navas, F.D., Damm, G., and Lamnabhi-Lagarrigue, F. (2015). Optimal power flow in multi-terminal HVDC grids with offshore wind farms and storage devices. *International Journal of Electrical Power and Energy Systems*, 65, 291 – 298.

Kundur, P., Balu, N.J., and Lauby, M.G. (1994). *Power system stability and control*. McGraw-Hill.

Lasseter, R.H. (2010). Microgrids And Distributed Generation. *Intelligent Automation and Soft Computing*, 16(2), 225–234.

Lifshitz, D. and Weiss, G. (2015). Optimal control of a capacitor-type energy storage system. *Automatic Control, IEEE Transactions on*, 60(1), 216–220. doi:10.1109/TAC.2014.2323136.

Löfberg, J. (2012). Automatic robust convex programming. *Optimization methods and software*, 27(1), 115–129.

Sandoval-Moreno, J., Besançon, G., and Martinez, J.J. (2013). Model predictive control-based power management strategy for fuel cell/wind turbine/supercapacitor integration for low power generation system. In *Power Electronics and Applications (EPE), 2013 15th European Conference on*, 1–10.

Zubieta, L.E. (2016). Are microgrids the future of energy?: DC microgrids from concept to demonstration to deployment. *IEEE Electrification Magazine*, 4(2), 37–44.